WRINKLE RIDGES AT THE LANDING SITE OF CHANG'E-3: POTENTIAL TARGETS TO REVEAL THE NATURE OF THRUST FAULTS ON THE MOON. Zhiyong Xiao[1], Zuoxun Zeng[1], Wenzhe Fa[2], Zhiyong Li[1], Long Xiao[1], Han Li[3], [1]China University of Geosciences (Wuhan), Hubei, 430074, P. R. China (zyxiao@cug.edu.cn). [2]Peking University, Beijing, 100871, P. R. China. [3]National Astronomical Observatories, Chinese Academy of Sciences, Beijing 100012, P. R. China.

Introduction: At December 14th 2013, the first Chinese soft-lander to the Moon, Chang'E-3 successfully touched the lunar surface at 19.51 ℃E, 44.12 ℃N, a mare surface within the Mare Imbrium. Four hours later, the rover Yutu (jade rabbit, named after a Chinese legend) was smoothly released from the lander, becoming the first man-made rover moving on the Moon since the end of the Apollo era back to 1970s.

As one of the seven payloads carried by Yutu, the two lunar penetration radars (LPRs) have different passband frequencies so that they can resolve subsurface structures of different depths and with various vertical resolutions along its paths. The high-frequency LPR is designed to resolve a minimum depth of 30 m and with a vertical resolution better than 30 cm, and the low-frequency LPR is able to detect subsurface features to a minimum depth of 100 m with a vertical resolution better than 10 m. Test data returned from the mission suggest that both the LPRs are functioning as well as designed.

We notice that wrinkle ridges vastly occur around the landing site and some of them may form in the Copernican era (<0.8 Ga [1]). Some of these features are located within the mobility radius of the Yutu rover. The subsurface structures of wrinkle ridges on the Moon (e.g., distribution and depth of faults, deformation of strata, and dip angles, etc.) are not well constrained but are critical in analyzing the stress condition when forming these features. Here we provide some potential targets for the LPRs to reveal the nature of thrust faults on the Moon.

Tectonic background: The most prominent tectonic features near the landing site are large wrinkle ridges (width>~5 km) that are radial or concentric to the center of the Imbrium basin (red lines in Fig. 1). These features formed after the emplacement of the mare basalts. Their poor preservation state suggests that faults formed these features have ceased activity for a long time. Both the sizes and the distributional pattern of these ridges are consistent with an origin caused by subsidence of the mare basalts filled in the Imbrium Basin [2]. One of these wrinkle ridges occurs about 10 km to the north of the landing site (Fig. 2a). It has a strike of about N–S and the southern end of the ridge terminates when encountering the younger basalt unit. Another large wrinkle ridge is visible ~20 km to the south of the landing site. It has a strike of about NW–SE and has extended into the younger mare units. Neither of these ridges is visible at the landing site (Fig. 2a).

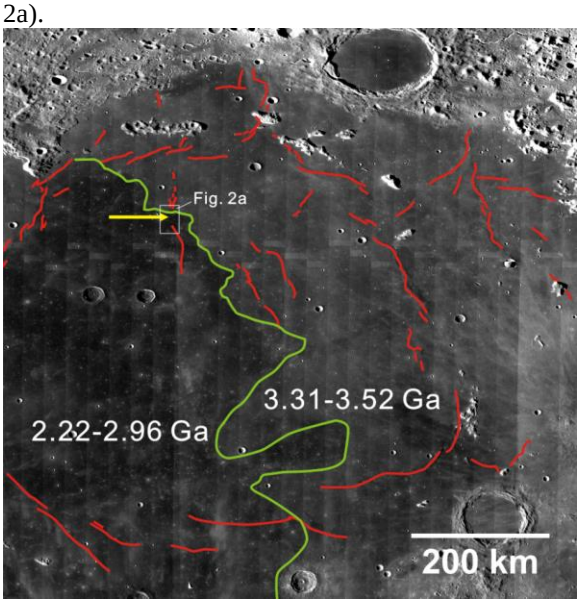

Fig.1. Distribution of major wrinkle ridges (red lines) within Mare Imbrium. The landing site of Chang'E-3 is pointed by the yellow arrow. The green line represents the approximate boundary between the two basalt units that filled the Imbrium basin. The two units have ages of 2.22–2.96 Ga and 3.31–3.52 Ga, respectively [3, 4]. The base image is from the LROC WAC global monochrome mosaic (100 m/pixel; equirectangular projection).

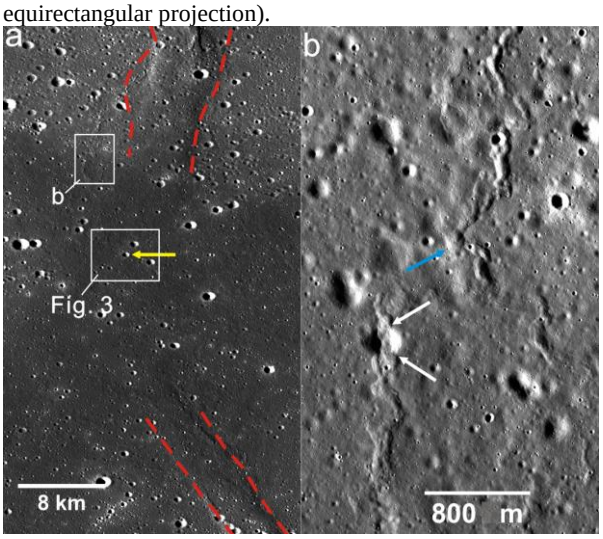

Fig. 2. Wrinkle ridges near the landing site (yellow arrow) of Chang'E-3. (a) Large wrinkle ridges that are over 5 km wide occur at both the south and north mare surface of the landing site, but they are not visible at the landing site. The base image is obtained by the Kaguya Terrain Camera

TCO_MAPm04_N45E339N42E342SC (~7.4 m/pixel; equirectangular projection). (b) Small wrinkle ridges that are less than ~2 km long and less than 400 wide deformed craters less than 100 m in diameter (while arrows). The wrinkle ridges have crisp morphology and craters less than 20 m in diameter (blue arrow) are transected by the ridges indicating these features are Copernican-aged compressional features. The base image is from LROC NAC M102285549LE and M102285549RE (1.71 m/pixel; sinusoidal projection).

Besides these large wrinkle ridges that might be associated with the subsidence of Mare Imbrium, many smaller wrinkle ridges are visible near the landing site. Some of them formed on top of the large wrinkle ridges, e.g., those shown in Fig. 2b. Such ridges are usually less than 2 km long and less than 400 m wide. They have very crisp morphology and craters having various preservation states are transected by these ridges. For example, the blue arrow in Fig. 2b shows a small crater ~20 m in diameter is transected by the wrinkle ridge. Compared with the survival time of small craters against surface erosion on the Moon [5], the observed crosscutting relationship between the small craters and the small wrinkle ridges suggests that these ridges formed in the Copernican era. Previous studies believed that late-stage global contraction of the Moon is the major cause for Copernican-aged compressional features on the Moon, of which most are lobate scarps [6, 7].

Potential targets for Yutu: Wrinkle ridges on planetary surfaces form in compressional stress conditions. After long controversies about their origin and possible subsurface structures, it is now widely accepted that their subsurface structures are similar with typical pop-up structures on Earth, which are mainly composed of a thrust fault, a recoil fault that has opposite trend with that of the thrust fault, and a broad anticline between the two faults [8]. However, no direct constraints of subsurface structures have ever been made for planetary wrinkle ridges, which largely affect the precise judgment of the stress condition in their formation and determining their possible stress sources.

The maximum mobility radius designed for the Yutu rover is ~3 km. Within this range limit, we propose some potential targets of wrinkle ridges for the LPRs to reveal the nature of thrust faults on the Moon.

The large wrinkle ridge. Large wrinkle ridge is not visible at the landing site. The assemblage pattern of the two large wrinkle ridges to the north and south of the landing site suggests that potential blind thrust faults that links the two wrinkle ridge may occur beneath the landing site (Fig. 2a). Alternatively, the two wrinkle ridges may form separately, in this case we wish to understand the subsurface structures in this transverse zone where the landing site is located. The relationship between the two periods of flood-basalts in the Imbrium Basin and the depth of the wrinkle ridges is also of great interest for understanding the tectono-magmatism evolutionary history of this region.

The small wrinkle ridge. Although the most prominent small wrinkle ridges in this region are ~5 km away from the landing site (Fig. 2a), we notice a small wrinkle ridge is located right to the north of the landing site (Fig. 3), which is within the mobility radius of the Yutu rover. The surface bulge caused by the wrinkle ridge is not as prominent as those shown in Fig. 2b, but we can still observe the relief difference between the ridge and the surrounding terrain. Small craters ~90 m in diameter is transected by the ridge. These observations suggest that the wrinkle ridge likely formed in late-Copernican, representing very recent tectonic features on the Moon. Alternatively, the ridge might be surface remnants of more ancient wrinkle ridges standing from long surface erosion. If the LPRs carried by Yutu would be able to delicately study the subsurface structures for this wrinkle ridge, we may be able to better constrain its identity and stress sources.

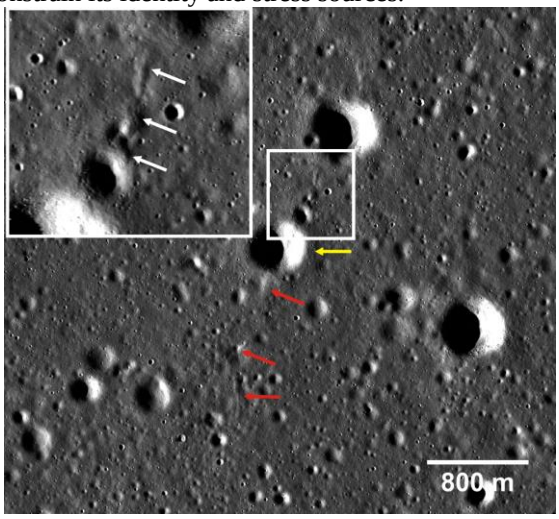

Fig. 3. A potential Copernican-aged wrinkle ridge at the landing site of Chang'E-3. The landing site is pointed by the yellow arrow. The inset is an enlargement for the wrinkle ridge to the north of the landing site and the red arrows denote possible traces of the wrinkle ridges. The base image is from LROC NAC M102285549LE and M102285549RE (1.71 m/pixel; sinusoidal projection).

References: [1] Stöffler D. and Ryder G. (2001) *SCR, 96*, 9–54. [2] Solomon S. C. and Head J. W. (1979) *JGR, 84*, 1667–1682. [3] Hiesinger H. et al. (2000) *JGR, 105*, 29239–29276. [4] Bugiolacchi R. and Guest (2008) *Icarus 197*, 1–18., Abstract #1402. [5] Trask N. J. (1971) *U. S. Geol. Surv. Prof. Pap.*750-D, D138. [6] Watters T. R. et al. (2010) *Science, 339*, 936–940. [7] Banks M. E. et al. (2012) *JGR*, E00H11. [8] Plescia J. B. and Golombek M. P. (1986) *GSAB, 97*, 1289–1299.